Glass-liquid transition of water at high pressure

Ove Andersson

Department of Physics, Umeå University, 901 87 Umeå, Sweden

Physical Sciences - Physics

PACS: 62.50.+p, 64.70.pF,65.60.+a

E-mail:ove.andersson@physics.umu.se

Phone:+46 90 7865034

Fax:+46 90 7866673

ABSTRACT

The knowledge of the existence of liquid water under extreme conditions and its concomitant properties are important in many fields of science. Glassy water has previously been prepared by hyperquenching micron-sized droplets of liquid water and vapour deposition on a cold substrate (ASW), and its transformation to an ultraviscous liquid form has been reported on heating. A densified amorphous solid form of water, high density amorphous ice (HDA), has also been made by collapsing the structure of ice at pressures above 1 GPa and temperatures below ~140 K, but a corresponding liquid phase has not been detected. Here we report results of heat capacity C_p and thermal conductivity, *in-situ*, measurements, which are consistent with a reversible transition from annealed HDA to ultraviscous high-density liquid water at 1 GPa and 140 K. On heating of HDA, the C_p increases abruptly by (3.4 ± 0.2) J mol^{-1} K^{-1} before crystallization starts at (153±1) K. This is larger than the C_p rise at the glass to liquid transition of annealed ASW at 1 atm, which suggests the existence of liquid water under these extreme conditions.

\body

Unlike most liquids that vitrify by normal supercooling, water vitrifies only by hyperquenching of its micron-size droplets and its porous amorphous state is made by vapor deposition (1,2,3). Pure bulk water densified by high pressure also does not vitrify on normal cooling, instead it freezes to proton-disordered high-density ices. However, in 1984 Mishima et al. (4) discovered a path to obtain a high-density amorphous ice (HDA) by pressurization of hexagonal ice, ice Ih, to ~1.5 GPa at 77 K. This amorphous form is characterized by the absence of Bragg peaks but it is heterogeneous on a mesoscopic length scale (5). On heating at high pressures above ~0.5 GPa (6), it relaxes, homogenizes and densifies before crystallization, and the ultimately densified form has been referred to as very high density amorphous ice (vHDA) (7). There are thus a multiplicity of amorphous states with densities in between HDA and vHDA, which are produced by isothermal pressurization of ice Ih at temperatures below ~140 K, and these are here generically referred to as HDA.

States of water at extreme pressure and temperature conditions are important for, e.g., understanding of tectonics in large bodies of the outer solar system where ice is one of the rock-forming minerals (8), and for water's phase diagram and properties (9), but it is not known whether HDA transforms to glassy and liquid states on heating. This work reports the first high-pressure, *in situ*, heat capacity C_p study of HDA just below its crystallization point where a glass to liquid transition may occur. It is here shown that HDA exhibits a glass transition with a heat capacity rise larger than that for amorphous solid water and hyperquenched water at 1 atm, which suggests a thermodynamic path between the annealed state of HDA and liquid water. The glass transition at 1 GPa is

observed as a sigmoid shape change in C_p and a peak in thermal conductivity for a time scale of ~1 s at 140 K.

Results and Discussion

Measurements were performed *in situ* by using the transient hot-wire method (see *Material and Methods* and *SI text*) that allowed for simultaneous measurement of heat capacity per unit volume, c, (or the product of the specific heat capacity and density), and thermal conductivity κ. About 17 ml of pure water was frozen in a Teflon cell (Fig. S1) placed inside a high pressure vessel, and the pressure raised to ~0.05 GPa. The sample was cooled to ~ 100 K, reheated and stabilized before it was pressurized isothermally at (129±1) K to 1.25 GPa at 0.1 GPa h^{-1} rate to collapse ice Ih to HDA. The results on cooling at 0.05 GPa agreed to within 2% with literature values (Fig. S2).

Fig. 1*A* shows that c of ice at 129 K gradually decreases linearly on pressurizing up to 0.7 GPa. This is the region in which ice lattice elastically deforms and the volume decreases while the phonon frequency increases, as generally observed for materials. The latter decreases c whereas the reduced volume increases c. On compression of ice up to a pressure of 0.7 GPa, the slowly decreasing c is due to the effect of pressure predominantly on the phonon frequency. On further compression, c rapidly decreases and reaches a local minimum at 0.84 GPa. As collapse of the ice structure begins, the initial increase in density decreases c rapidly as a premonitory occurrence to its full collapse, after which decompression does not restore the original structure of ice. Neutron scattering studies (10) have shown that as structural collapse occurs, extra H_2O molecules are forced to move into

the first coordination shell of the hydrogen bonded four near neighbors of a reference H_2O molecule. The density increases initially gradually, but the phonon frequency increases much more rapidly. The overwhelming effect of the latter causes *c* to decrease rapidly. In the pressure range 0.85 - 1.0 GPa, the structure strongly densifies as the extra H_2O molecules enter their (interstitial) sites in first coordination shell.[*] The resulting large and irreversible increase in density dominates, and *c* increases rapidly as the structure ultimately collapses with increasing pressure to HDA, which has a structure similar to that of high-density liquid water (10,11). On further compression, the collapsed structure homogenizes with a likely overall increase in the diffusion time. The consequence of such an increase near a glass transition would be an irreversible decrease of *c*, like that observed here in the 1 to ~1.15 GPa range, until the homogenization approaches completion (see also *SI text*). In this process, the orientationally-disordered structure of ice (12) converts to a canonically disordered structure of hydrogen-bonded and interstitial H_2O molecules, i.e. a state with no long-range translational periodicity, that transforms ultimately to a kinetically-frozen state, as measured on a 1 s time scale (see *Material and Methods* and *SI text*). Because of the heterogeneous character of the state initially formed at 1.2 GPa (5) and its subsequent further relaxation and homogenization during heating, it appears similar to the high-energy state of a collapsed crystal obtained by mechanical deformation (13).

[*] Neutron diffraction data for samples recovered at 1 atm and 77 K suggest that there are approximately two interstitial H_2O molecule in vHDA, and one in HDA produced at 77 K (10).

Fig. 1*B* shows the concurrent change in κ on pressurizing ice at 129 K. The κ decreases linearly with increasing pressure until ~ 0.75 GPa, and then more abruptly in the pressure range of 0.8 - 1 GPa. The latter decrease is due to the structural collapse of ice that decreases the mean free path for propagation of phonons, *l*. This decrease dominates the changes in the parameters of the Debye's approximate relation (14), $\kappa = cvl/3$ where *v* and *c* are the velocity and heat capacity per unit volume of the heat-carrying phonons. After a sigmoid shape decrease, κ reaches a plateau like value of 0.66 W m^{-1} K^{-1} at ~1.15 GPa, thereby indicating that the structural collapse of ice is approaching completion.

The sample was then heated from 100 K to 148 K at 0.4 K min^{-1} rate and subsequently cooled to 100 K at 0.3 K min^{-1} at 1 GPa before reheating. On first heating of the collapsed state at 1 GPa, κ increases in a broad sigmoid shape manner (Fig. 2*B*), as the state relaxes to a lower energy and the structure densifies. On cooling from 148 K, the slope becomes negative and a peak appears at 140 K. On subsequent heating, κ retraces its path and a peak reappears at 140 K. This shows that the results become reversible after the first heating to 148 K, which yields the state referred to as vHDA (7). Moreover, the peak or change in the sign of $d\kappa/dT$ at 140 K is typical for the onset of kinetic-unfreezing on heating and of kinetic-freezing on cooling. It is commonly observed at glass-liquid transitions, and is generally reported for e.g. those of polymers (15). It likely occurs mainly as a result of a change in the thermal expansivity. On further heating, κ increases rapidly showing that crystallization began at (153±1) K, and this exothermic process was also detected by an accelerated rate for the sample temperature increase, as shown in Fig. 2*A* (see *SI text* for a detailed analysis of the crystallization temperature).

In the plot of the measured *c* of the relaxed state at 1 GPa (second heating), shown by the circles in Fig. 3*A*, a sigmoid-shape increase appears with onset at 140 K. This is a characteristic feature of a glass transition which shows the temperature range of kinetic unfreezing, and from which the glass transition temperature T_g is determined. Since the density of the annealed state at 1 GPa changes by less than 1% over the temperature range of interest, the plot of *c* is effectively the plot of C_p, the specific heat per mole. To show the sigmoid-shape change more clearly, *c* in Fig. 3*A* was converted to C_p by using the HDA's density of 1.35 g cm^{-3} at 1.2 GPa in the 130-140 K range (16), and the difference between the measured C_p and the linearly extrapolated (vibrational) C_p from the glassy state plotted in Fig. 3*B*.

Fig. 3*B* shows that the heat capacity increase at T_g is (3.4±0.2) J mol^{-1} K^{-1} before the sluggish crystallization affects the results above ~153 K. This rise thus occurs within a temperature range of about 13 K. Although the increase tends to level off, C_p still rises when crystallization interferes with the results, which indicates that the glass transition range extends a few degrees further and that the heat capacity step is somewhat larger than (3.4±0.2) J mol^{-1} K^{-1}. The time scale of the method is about 1 s, which means that the (average) relaxation time of the motions associated with the glass transition is less than ~1 s at the onset temperature of the C_p rise. On further temperature increase, their contribution to the measured C_p increases as the relaxation time decreases. Finally, at a temperature well above T_g where the relaxation time is much less than 1 s, the increase in C_p levels off as the configurational degrees of freedom, which are frozen at T_g, equilibrate quickly. This change in the heat capacity contribution of the configurational modes can be calculated as a function of relaxation time, or temperature, by an analysis of the method. The total heat

capacity step can therefore be estimated and the analysis indicates that ~90% of the heat capacity step has occurred when crystallization intervenes at 153 K (*see SI text*). It follows that the estimated heat capacity rise in the entire glass transition range is (3.7±0.4) J mol^{-1} K^{-1}, where the uncertainty of ~10% includes also an uncertainty in the subtracted vibrational heat capacity.

The results for HDA can be compared with those for the glass transitions of vapor-deposited amorphous solid water (ASW) (2) (see Fig. S3) and hyperquenched glassy water (HGW) (3) at 1 atm. In these cases, crystallization interferes at a temperature about 14 K above T_g and the C_p increases in this range are (1.9 ± 0.2) J mol^{-1} K^{-1} (2) and (1.6 ± 0.2) J mol^{-1} K^{-1} (3) for the glass-liquid transition of ASW and HGW, respectively.[†] (In a later study (17), a smaller value of 0.7 J mol^{-1} K^{-1} was reported for HGW.) Thus, the heat capacity rise for HDA is larger. It is also larger than the C_p rise of 0.7 J mol^{-1} K^{-1} (18) and (1.8± 0.2) J mol^{-1} K^{-1} (19) at T_g of the low density amorphous ice, which forms from HDA on heating to ~125 K at 1 atm.

The C_p rise at 140 K shows that there is an increase of configurational degrees of freedom,[‡] which is normally associated with both translational and rotational diffusion. A dielectric spectroscopy study (20) has already shown the presence of reorientational

---

[†] T_g of water is debated, but in a review by Debenedetti (9) it was concluded that most experimental observations support T_g=136 K and, thus, that the C_p step at T_g of ASW and HGW are 1.9 J mol^{-1} K^{-1} and 1.6 J mol^{-1} K^{-1}, respectively.

[‡] The change in the heat capacity at T_g may also include a change in the vibrational part, but the major change is due to configurational modes.

motions with a relaxation time of ~ 0.3 s at 140 K (20,21), which is in good agreement with the C_p results (see Fig. S3 and *SI text*). In principle, the dielectric results could be due to an orientational glass transition, i.e. a transition from a state with frozen-in orientational disorder to one with reorientational motions. Haida et al. (22) have established such a transition for crystalline proton-disordered ice Ih, and it may occur in all proton-disordered crystalline phases of ice. However, a corresponding transition here can be excluded on the basis of the amorphous structure of HDA (10,11), and the size of the C_p increase. In the case of ice Ih (22), the C_p increase at the glass transition was small and difficult to detect even in high-accuracy adiabatic calorimetry. The C_p change observed here is larger than that for the glass to liquid transition at 1 atm, which implies that the transition cannot be associated with fewer configurational degrees of freedom than those of the glass to liquid transition. Consequently, when the glassy state at 1 GPa is heated, *c* indicates that the onset of structural fluctuations by diffusion on the time scale of ~ 1 s occurs at 140 K. On further heating, *c* of apparently ultraviscous water at 1 GPa increases rapidly as its entropy increases with increase in the structural fluctuations rate. The resulting decrease in viscosity increases the diffusion-controlled crystallization rate, and water at 1 GPa begins to crystallize at (153±1) K. In contrast to the usual calorimetry, which shows crystallization as a local sharp minimum in the measured C_p, the technique used here shows the crystallization as a local peak in the measured *c* (see *SI text*). The subsequent variation of *c* with temperature, shown in Fig. 3*A*, is typical of a completely crystallized solid.

The common behavior of easily crystallizing liquids on heating from the glassy state is structural relaxation and a glass to liquid transition followed by crystallization, i.e. the same behavior as observed here on heating of HDA at 1 GPa. Moreover, Mishima (23) has

studied the nature of isothermal pressure collapse of ice Ih and found "..a smooth cross-over from (pressure induced) equilibrium melting to sluggish amorphization at around 140-165 K. ", which seems consistent with the results here that HDA apparently becomes an ultraviscous liquid before crystallization at about 153 K on slow heating at 1 GPa. The results are also consistent with computer simulations that indicate a link between the annealed HDA and quenched high pressure liquid water (24).

During the reviewing process of this work, Seidl *et al.* [25] have reported a study of volume expansion of HDA and suggested that HDA crystallizes before its glass transition at pressures above 0.4 GPa, but shows a glass transition below 0.4 GPa. Moreover, Seidl *et al.* [25] discuss results to be published, which suggest a calorimetric glass transition near 115 K at 1 atm. It appears feasible that the glass transition observed here at 140 K and 1 GPa on a time scale of ~1 s can occur at 115 K and 1 atm on a longer time scale.

Conclusions.

Compression of ice at ~130 K to ~1.3 GPa slowly collapses it to a topologically disordered solid. On heating at 1 GPa, the structure of the solid relaxes and the relaxed state shows a glass transition with a heat capacity increase larger that for the glass to liquid transition at 1 atm. This suggests that the collapsed ice state transforms to liquid water on heating, which vitrifies on subsequent cooling or, in other words, that glassy and liquid water are connected by a reversible path under these extreme conditions. This high density state of water is apparently favorable for suppressing crystallization, which does not occur until the relaxation time becomes less than 10^{-2} s. The relatively sluggish crystallization kinetics promotes further studies of water's properties in its ultraviscous high-density state than is possible for the rapidly crystallizing ultraviscous liquid water at 1 atm. Moreover, since ice

is one of the rock-forming minerals in the outer Solar system and most of the ice moons of Jupiter and Saturn have had some form of tectonic or internal activity, one expects that this activity would have been greatly affected by the glass transition of water with temperature change at high pressures (8). The glass transition at 1 GPa is also essential for progressing the knowledge of water's phase diagram, which may include two liquid water phases of different densities that have a common phase coexistence line at low temperatures (9). The results reported here imply the existence of at least one of these, a low-temperature high-density liquid water phase.

Material and methods

Measurements were performed *in situ* by using the transient hot-wire method (see *SI text* for details). Pure water (Milli-Q® Ultrapure WaterSystems) was frozen in a 14 mm deep, 39 mm internal diameter Teflon sample cell placed inside a high pressure vessel of ~1.5 GPa capacity. The Teflon sample cell contained a 0.3 mm diameter and 40 mm long Ni wire (hot-wire) in the form of a circular loop that allowed simultaneous measurement of the heat capacity per unit volume, c and thermal conductivity κ. The hot-wire, surrounded by the frozen water, was heated by a ~1 s long pulse of nominally constant power, and its electrical resistance was measured as a function of time. The wire acted as both the heater and the sensor for the temperature rise, which was calculated by using the relation between its resistance and temperature. The analytical solution for the temperature rise with time was fitted to the data points for the hot-wire temperature rise thereby yielding both c and κ.

ACKNOWLEDGEMENTS. I thank G. P. Johari and H. Suga for encouraging me to look into this problem and for discussions.This work was supported financially by the Faculty of Science and Technology, Umeå University.

References

1. Burton E F, Oliver W F (1935) X-Ray Diffraction Patterns of Ice. *Nature* 135: 505-506.
2. Hallbrucker A, Mayer E, Johari G P (1989) Glass-liquid Transition and the Enthalpy of Devitrification of Annealed Vapor-Deposited Amorphous Solid Water. A Comparison with Hyperquenched Glassy Water. *J. Phys. Chem.* 93: 4986-4990.
3. Johari G. P, Hallbrucker A, Mayer, E (1987) The glass-liquid transition of hyperquenched water. *Nature* 330: 552-553.
4. Mishima O, Calvert L D, Whalley E (1984) "Melting" ice at 77 K and 10 kbar: a new method of making amorphous solids. *Nature* 310: 393-395.
5. Koza M M, Hansen T, May R P, Schober H (2006) Link between the diversity, heterogeneity and kinetic properties of amorphous ice structures, *J. Non-Cryst. Sol.* 352: 4988-4993.
6. Salzmann C G, Mayer E, Hallbrucker A (2004) Effect of heating rate and pressure on the crystallization kinetics of high-density amorphous ice on isobaric heating between 0.2 and 1.9 GPa, *Phys. Chem. Chem. Phys.* 6: 5156-5165.
7. Loerting T, Salzmann,C, Kohl I, Mayer E, Hallbrucker A (2001) A second distinct structural ``state" of high-density amorphous ice at 77 K and 1 bar. *Phys. Chem. Chem. Phys.*, 3: 5355-5357.

8. Poirier J P (1982) Rheology of ices: a key to tectonics of the ice moons of Jupiter and Saturn. *Nature* 299: 683-687.

9. Debenedetti P G (2003) Supercooled and glassy water, *J. Phys. Condens. Matter.* 15: R1669-R1726.

10. Finney J L, Bowron D T, Soper A K, Loerting T, Mayer E, Hallbrucker A (2002) Structure of a New Dense Amorphous Ice, *Phys. Rev. Lett.* 89: 205503.

11. Finney J L, Hallbrucker A, Kohl I, Soper A K, Bowron D T (2002) Structures of High and Low Density Amorphous Ice by Neutron Diffraction. *Phys. Rev. Lett.* 88: 225503 (2002).

12. Suga H, Matsuo T, Yamamuro O (1992) Thermodynamic study of ice and clathrate hydrates. *Pure & Appl. Chem.* 64: 17-26.

13. Johari G P, Andersson O (2007) Vibrational and relaxational properties of crystalline and amorphous ices. *Thermochim. Acta* 461: 14-43.

14. Berman R (1949) Thermal Conductivity of Glasses at Low Temperatures. *Phys. Rev.* 76: 315-316.

15. Van Krevelen D (1972) *Properties of Polymers* (Elsevier, Amsterdam) pp. 233.

16. Mishima O (1994) Reversible first-order transition between two H_2O amorphs at ~0.2 GPa and ~135 K. *J. Chem. Phys.* 100: 5910-5912.

17 Kohl I, Bachmann L, Mayer E, Hallbrucker A, Loerting T (2005) Glass transition in hyperquenched water? *Nature* 435: E1.

18. Handa Y P, Klug D D (1988) Heat Capacity and Glass Transition Behavior of Amorphous Ice. *J. Phys. Chem.* 92: 3323-3325.

19. Johari G P, Hallbrucker A, Mayer E (1996) Two Calorimetrically Distinct States of Liquid Water Below 150 Kelvin. *Science* 273:90-92.

20. Andersson O (2005) Relaxation Time of Water's High-Density Amorphous Ice Phase, *Phys. Rev. Lett.* 95: 205503.

21. Andersson O, Inaba, A (2006) Dielectric properties of high-density amorphous ice under pressure. *Phys. Rev. B* 74: 184201.

22. Haida O, Matsuo T, Suga H, Seki S (1974) Calorimetric study of the glassy state X. Enthalpy relaxation at the glass-transition temperature of hexagonal ice, *J. Chem. Thermodyn.* **6**: 815-825.

23. Mishima O (1996) Relationship between melting and amorphization of ice. *Nature* 384: 546-549.

24. Giovambattista N, Stanley H E, Sciortino F (2005) Relation between the High Density Phase and the Very-High Density Phase of Amorphous Solid Water. *Phys. Rev. Lett.* 94: 107803.

25. Seidl M, Elsaesser M. S., Winkel K, Zifferer G, Mayer E, Loerting T (2011) Volumetric study consistent with a glass-to-liquid transition in amorphous ices under pressure, *Phys. Rev. B.* 83: 100201.

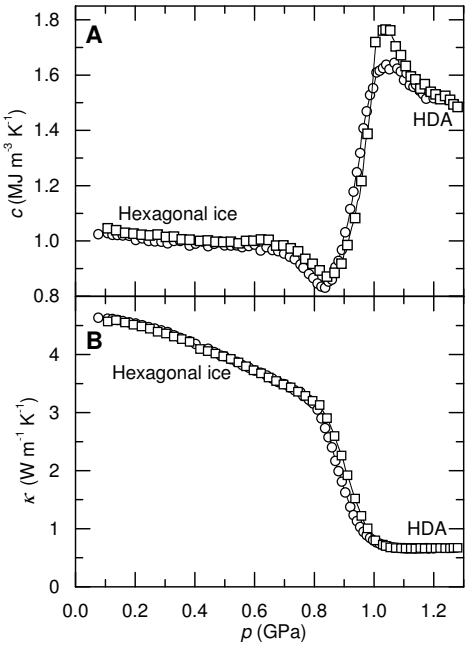

Fig. 1. Thermal properties prior, during and after pressure collapse of hexagonal ice, ice Ih. (*A*) Heat capacity per unit volume, and (*B*) Thermal conductivity on isothermal pressurization at (129±1) K. The squares and circles show results for two different runs, which agree to within 2% outside the collapse range.

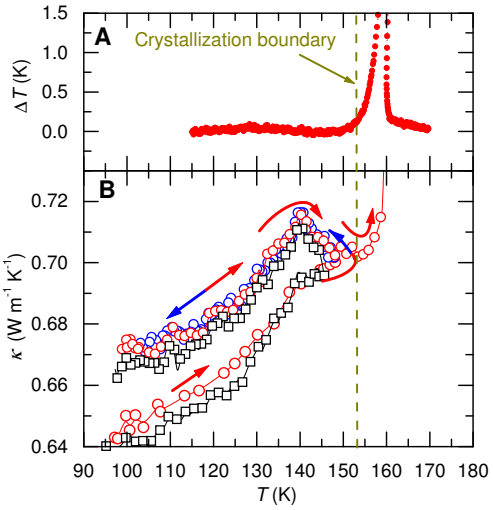

Fig. 2. Relaxation behavior, reversible glass transition and crystallization. (*A*) Excess sample temperature, which was obtained by subtracting a function fitted to measured data for temperature vs. time below 140 K and above 165 K, during heating at 1 GPa. (*B*) Thermal conductivity during heating from 100 to 148 K, cooling from 148 to 100 K, and reheating to 175 K at 1 GPa. On the first heating to 148 K, the collapsed ice relaxes and apparently transforms to ultraviscous high-density liquid water at 140 K, which vitrifies on cooling. The squares and circles show results for two different runs. The increase in κ at ~153 K is due to sluggish crystallization.

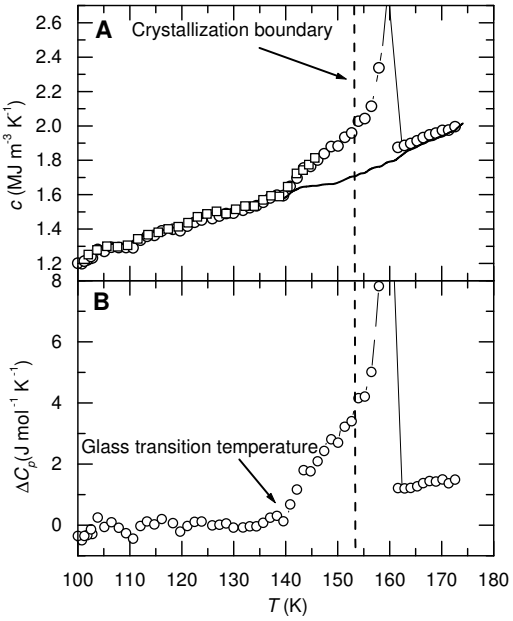

Fig. 3. Glass transition on heating at 1 GPa. (*A*) Heat capacity per unit volume of glassy water, its kinetically unfrozen state and crystallized ice (line on cooling) at 1 GPa. The squares and circles show results for two different HDA samples on heating. (In one of the runs the sample was heated only to 146 K and then cooled.) (*B*) Excess molar heat capacity plotted against temperature at 1 GPa. Results on heating after the sample had been pretreated by heating to 148 K at 0.4 K min^{-1} and cooled to 100 K at 0.3 K min^{-1}. At these heating and cooling rates, HDA slowly annealed to its ultimate high-density state, which has a T_g of ~140 K measured on a 1 s time scale.

Supporting Information

Glass-liquid transition of water at high pressure

O. Andersson

SI Text.

Supplementary Method Description. Heat capacity per unit volume c (the product of density and specific heat per unit mass) and thermal conductivity κ were measured *in situ* by using the transient hot-wire method (1,2). Briefly, a 0.3 mm Ni-wire (the "hot-wire") was heated by a square pulse of 1.4 s duration and q Watts per unit length (see Fig. S1 for sample cell arrangement). It raised the wire's temperature by ~3.5 K in a time dependent manner which is determined by c and κ of the sample. The increase was measured with time as a change in the resistance between two electrical potential taps on the hot-wire itself. In the approximation of infinite length of the wire, the heat transfer equations for the wire and the surrounding solid are given by:

$$\frac{\partial^2 T}{\partial r^2} + \frac{1}{r}\frac{\partial T}{\partial r} - \frac{1}{a_w}\frac{\partial T}{\partial t} = -\frac{q}{\kappa_w \pi r_w^2} \qquad [S1]$$

$$\frac{\partial^2 T}{\partial r^2} + \frac{1}{r}\frac{\partial T}{\partial r} - \frac{1}{a}\frac{\partial T}{\partial t} = 0$$

where t and T are time and temperature, r is the radial co-ordinate, κ_w is the thermal conductivity of the wire, a and a_w are the thermal diffusivity of sample and the wire

respectively. The exact solution of the temperature rise ΔT of an infinitely long, infinitely conducting wire immersed in an infinitely large sample is (3)

$$\Delta T = \frac{2q\alpha^2}{\pi^3\kappa}\int_0^\infty \frac{1-\exp(-\beta u^2)}{u^3\left\{(uJ_0(u)-\alpha J_1(u))^2+(uY_0(u)-\alpha Y_1(u))^2\right\}}du, \qquad [S2]$$

where $\alpha=2c/c_w$, $\beta=\kappa t/(c\, r_w^2)$, r_w is the radius of the wire, c_w is the heat capacity per unit volume of the hot-wire, J_0 an J_1 are Bessel functions of the first kind of zero and first order, Y_0 and Y_1 are Bessel functions of the second kind of zero and first order.

A fit of Eq. S2 to the measured temperature rise of the hot-wire yields both c and κ. Measurements showed that with the 0.3 mm diameter hot-wire used here, c values of ice measured at $T > 120$ K, were within 2% of the value determined by adiabatic calorimetry data, as seen in Fig. S2. The pressure was determined from the known load per unit area and corrected for friction. The temperature was measured with a chromel alumel thermocouple immersed in the sample. Their uncertainties are 0.05 GPa and 0.5 K. The measured κ has an uncertainty of $\pm$ 2%.

Hot-wire results near a glass transition. On heating through the glass to liquid transition, the non-equilibrium state of the glass kinetically unfreezes and the resulting gain in the configurational part of c appears as a sigmoid-shape increase in the plot of c against T. As is well-known, the glass transition temperature varies with the time scale used to analyze the response of heat exchange with the sample. In the hot-wire analysis of a response to a 1.4 s heating pulse, as the sample is simultaneously heated or cooled slowly by the surroundings at a rate less than 0.5 K min^{-1}, the measured kinetic unfreezing occurs on a time scale of ~1 s (transient heating rate of 3.5 K in 1.4 s or 150 K min^{-1}). Thus, the slow

heating or cooling rate caused by the surroundings does not affect the position of the sigmoid-shape increase in the temperature plane. This time scale is much shorter than that of adiabatic calorimetry where the sample is also heated by a transient pulse but the analysis requires a long-time waiting time of several minutes to reach equilibrium. The technique differs also from differential scanning calorimetry (DSC) where the temperature of the sigmoid-shape heat capacity C_p increase is determined by the heating and cooling rates. Measurement of κ commonly shows a peak at a glass transition (6), i.e., a change in the sign of $\mathrm{d}\kappa/\mathrm{d}T$, as is also observed here for the annealed state of collapsed ice (HDA).

When a sample crystallizes on heating, the temperature of the sample rises and in the DSC technique, the resulting heat loss appears as an anomalous decrease in c with increasing T. Crystallization also affects the measurements done here but appears as an anomalous (irreversible) *increase* in c. This stems from the manner of crystal growth that occurs generally at random sites in the sample, but since the temperature rise and decay begins at the hot-wire probe in this technique the wire acts not only as a nucleation site but also as a site of preferred growth. Moreover, the exothermic process increases the temperature rise of the wire probe. A finite element analysis by using Eq. S1 and subsequent fitting of Eq. S2 showed that c increases artificially when an ice layer forms on the probe and when the wire probe is heated by the exothermic process. Decrease in C_p observed on heating in DSC is also an artefact, and is useful for determining the enthalpy loss from the $C_p\,\mathrm{d}T$ integral. This is not possible by this technique, but it opens the possibility of studying glassy water and its transition by measuring changes in thermodynamic properties when other methods are not usable at high pressures.

Comparison with previous results. Previously reported dielectric spectroscopy results [7,8] show that a relaxation process can be detected in the dielectric data on heating of the high density amorph at 1 GPa (Fig. S3). Thus, dielectric results suggest that there is a glass transition in the high density amorph. This is an important result, which strongly corroborates that the heat capacity increase observed here at 140 K is also due to a glass transition. Fig. S3 shows a comparison between the dielectric loss ε'' at 0.16, 3 and 10 Hz and the heat capacity measured on heating at 1 GPa. The rise in the heat capacity occurs at 140 K for a time scale t_{HW} of *about* 1 s. This means that if the temperature of maximum loss at ~0.16 Hz (=1/(2*π*t_{HW})) occurs near 140 K, then the heat capacity rise and the dielectric loss peak are most likely due to the same process. The results shown in Fig. S3 verify that this is the case.

Fig. S3 also shows heat capacity results for vapor-deposited amorphous solid water $(ASW)^{measured}$ using DSC at 1 atm [9]. The data for ASW have been inserted for comparison to demonstrate that these are similar as those of the relaxed high density amorph. ASW shows a broad glass transition and the crystallization occurs only slightly above the glass transition temperature. The high pressure data show a somewhat more abrupt onset and a larger increase.

Crystallization temperature and heat capacity increase at the glass transition temperature T_g. To accurately establish the heat capacity increase at T_g, it is necessary to determine the temperature at which crystallization affects the results by growth of a thin ice layer on the probe, as described above. This was done through a systematic study using temperature cycles at 1 GPa. However, the experiments on pressure-amorphization of ice in

this high-pressure assembly are particularly prone to failure because the slow rate of pressurization, large sample volume and/or in-situ measurements causes the amorphous solid-ice Ih mixture to frequently crystallize in the broad pressure amorphization range of 0.8 GPa to 1.1 GPa. Moreover, the probe wire occasionally breaks. An average of less than one in five attempts to amorphized a sample, each requiring at least three days, is successful. To practically enable the study, water doped with tetrahydrofuran (THF) (less than 0.5 mol%) was tested after seven consecutive failures, and since the first attempt succeeded it probably reduced the tendency of abrupt crystallization during the amorphization process.

The collapsed state of this sample was formed by slow pressurization at 130 K up to 1.2 GPa. The pressure was thereafter decreased to 1 GPa at which the sample was temperature cycled several times, where each cycle refers to a heating run to above T_g and a subsequent cooling run to a temperature well below T_g (typically below 115 K). The sample was first cycled three times to a temperature in the range 147-148 K, thereafter once to 149 K and 151 K, respectively, and then finally to 153.5 K. As shown in Fig S4, only the final temperature cycle to 153.5 K gave irreversible results, which were caused by slow crystallization. (Calculations, as described above, indicate that a ~5 μm thin crystalline ice layer had formed on the wire probe. This thin ice layer causes an about 7 % anomalous irreversible increase in c like that observed in the measurements, but only a 0.8% anomalous decrease in κ. The experimental results of κ are essentially unaffected, which is likely due to slight crystal growth in the sample that gives a real increase that counteracts the anomalous decrease. Since the sample remains almost 100 % amorphous, the glass

transition feature still appears in both c and κ on cooling.) Due to the large heat capacity of the vessel, which gives sluggish changes from heating to cooling as well as slow heating and cooling rates, these numerous cycles meant that the sample had spent about 7 h above T_g before crystallization was observed in the range 151-153.5 K. The results for the cycle up to 151 K were reversible and therefore not subjected to error caused by slow crystallization on the wire probe despite that the sample remained ~20 min within 0.5 K of 151 K during the temperature cycle. The maximum excess heat capacity for the 151 K cycle agrees with that obtained at about 153 K on continuous heating of pure water using 0.4 K/min rate. Moreover, at about 153 K, the thermocouple recording indicated an exothermic process on continuous heating of the pure water sample (Fig. 2A). Thus, these data combined show that pure ice crystallized at (153±1) K on continuous heating and that the heat capacity data rise below this temperature is due to the glass transition and not subjected to error due to slow crystallization on the probe.

The data for c indicates a levelling off at 153 K before crystallization interrupts giving an anomalous increase. The extent to which c would further increase unless crystallization intervened, can be studied using a model for the time-dependence, or frequency dependence [10], of the heat capacity in the glass transition range. In a simplified description, the heat capacity per unit volume varies with time as:

$$c(t) = c_\infty + (c_0 - c_\infty)\, e^{-(t/\tau)^\beta} \qquad \text{[S3]}$$

where c_0 and c_∞ are the short and long time values associated with the glass and liquid states, respectively, τ is the relaxation time and β is an exponent between 0 and 1. That is, the total increase in c due to the glass transition is given by c_∞ - c_0. By inserting Eq. S3 in

Eq. S1, the temperature rise of the wire probe can be calculated for a given relaxation time. A subsequent fit of Eq. S2 yields c and, thus, the fraction of c_∞ - c_0 which is measured by the method for a given relaxation time. The values of c_0 and c_∞ were chosen based on the experimental values but since we are here interested to determine the fraction of the total increase as a function of relaxation time, their magnitudes are not critical. A very short relaxation time gives the liquid $c = c_\infty$ whereas a long relaxation time gives the glassy $c = c_0$. The shape of the rise depends on β and β=0.5 gave good agreement with the experimental data, as shown in Fig S5. The values of τ for the measured heat capacity increase $\triangle C_p$ versus temperature were calculated from dielectric relaxation time data versus temperature [8]. The calculated c (or C_p) rise and the measured rise occur at slightly different τ, as shown in Fig. S5. The shift in log (τ) of about 0.4 corresponds to a temperature difference of ~3.5 K, which indicates that there is only a slight difference between the dielectric and calorimetric relaxation times of HDA. The results for the calculated C_p rise in Fig. S5 have been scaled vertically to best coincide with the experimental values. The dashed lines provide an error estimate of 10% in the C_p rise, which includes also an uncertainty in the baseline used to subtract the vibrational part of the experimental heat capacity. (The scaling procedure assumes that the temperature dependence of the dielectric and calorimetric relaxation times is roughly the same in the transition range.) The results indicate that ~90% of the total rise (c_∞ - c_0) has occurred when crystallization intervenes. In other words, if crystallization can be prevented, these calculations indicate that the contribution from kinetic unfreezing of molecular motions at T_g would increase C_p further and give a total heat capacity increase of (3.7±0.4) J mol^{-1} K^{-1} in the glass transition range.

Heat capacity change during the collapse. In order to study the behaviour of *c* during collapse at lower temperatures, several attempts were made to collapse ice Ih in the 110-120 K range, but all failed due either to abrupt crystallization or probe failure. However, data using a 0.1 mm hot-wire probe were obtained at 115 K in a study in 2004 [11], which is the only successful attempt to measure the thermal properties during the collapse in this temperature range. The 0.1 mm probe gives erroneous results for *c* of ice Ih due to its high thermal diffusivity and does not provide the high accuracy for the collapsed state as shown here using a 0.3 mm probe. (The 0.3 mm probe gives a better description of the initial temperature rise of the hot-wire probe, which is important for obtaining accurate values for *c*, as discussed in more detail in Ref. [1].) Despite the lower accuracy, these should indicate the changes in *c* during the latter part of the collapse where the thermal diffusivity is relatively low. The data are shown in Fig S6, together with the high accuracy data obtained during collapse at 130 K. The 115 K data do not show a clear peak in the data up to 1.3 GPa as that observed in *c* at 130 K, which indicate that the collapse at low temperatures proceeds differently than at 130 K and support that the peak in *c* at 130 K is due to homogenization of the sample.

1. Håkansson B, Andersson P, Bäckström G (1988) Improved hot-wire procedure for thermophysical measurements. *Rev. Sci. Instrum*. 59: 2269-2275.
2. Andersson O, Inaba, A (2005) Thermal conductivity of crystalline and amorphous ices and its implications on amorphization and glassy water, *Phys . Chem. Chem. Phys*. 7: 1441-1449.

3. Carslaw H S, Jaeger J C (1959) *Conduction of heat in solids* 2nd ed. (Clarendon, Oxford), pp. 341.

4. Giauque W F, Stout J W (1936) The Entropy of Water and the Third Law of Thermodynamics. The Heat Capacity of Ice from 15 to 273.0 K. *J. Am. Chem. Soc.* 58: 1144-1150.

5. Hobbs P V (1974) *Ice Physics* (Clarendon Press, Oxford).

6. Van Krevelen D (1972) *Properties of Polymers* (Elsevier, Amsterdam), pp. 233.

7. Andersson O (2005) Relaxation Time of Water's High-Density Amorphous Ice Phase, *Phys. Rev. Lett.* 95: 205503.

8. Andersson O, Inaba A (2006) Dielectric properties of high-density amorphous ice under pressure. *Phys. Rev. B* 74: 184201.

9. Hallbrucker A, Mayer E, Johari G P (1989) Glass-liquid Transition and the Enthalpy of Devitrification of Annealed Vapor-Deposited Amorphous Solid Water. A Comparison with Hyperquenched Glassy Water. *J. Phys. Chem.* 93: 4986-4990.

10. Birge N O, Nagel S R (1985) Specific-Heat Spectroscopy of the Glass Transition, Phys. Rev. Lett. 54, 2674–2677.

11. Johari G P, Andersson O (2004) Mechanisms for pressure- and time-dependent amorphization of ice under pressure. *Phys. Rev. B* 70: 184108.

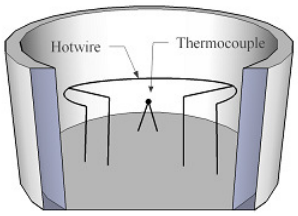

Fig. S1. Teflon sample cell with the hot-wire probe and thermocouple for high-pressure in-situ measurements of thermal conductivity and heat capacity per unit volume.

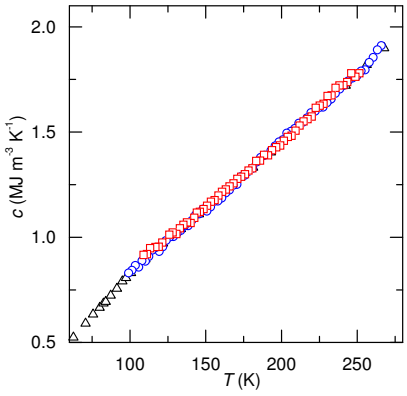

Fig. S2. Heat capacity per unit volume of hexagonal ice at ~0.05 GPa plotted against the temperature. (□) and (○) are the data obtained in two experiments by using 0.3 mm diameter hot-wires. (△) are the values determined from C_p data (4) and density (5). At $T >$ 120 K, the values agree to within 2%. At $T <$ 110 K, interference with the reflection of the heat wave from the cell wall added to the uncertainty in the measurements.

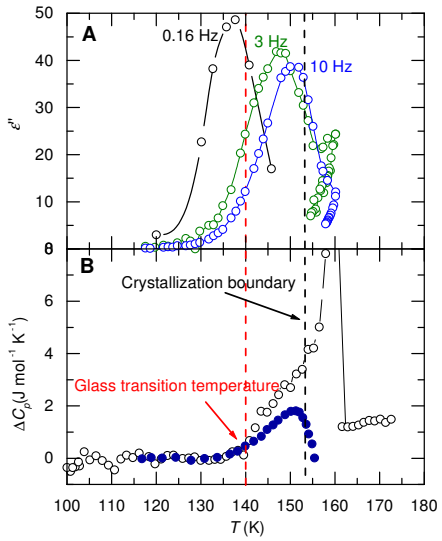

Fig. S3. Glass transition and crystallization on heating at 1 GPa. (*A*) Dielectric loss ε'' plotted against temperature for three different frequencies: 0.16 Hz, 3 Hz and 10 Hz. The results at 3 and 10 Hz were measured on continuous slow heating at ~0.3 K/min (previously unpublished). The results at 0.16 Hz pertain to a different water sample and were obtained from frequency scans at constant temperature, either directly from the measured results (at 138 K and below) or by extrapolation based on superposition of the spectrum at 138 K on spectra measured for frequencies above 3 Hz [7,8] (at 141 K and above). The sizes of ε'' are rough due to the uncertainty in the cell dimensions but this does not affect the temperature of maximum loss. (*B*) Excess molar heat capacity plotted against temperature at 1 GPa. Results on heating after the sample had been pretreated by heating to 148 K at 0.4 K min^{-1} and cooled to 100 K at 0.3 K min^{-1}. The filled circles are results for vapor-deposited amorphous solid water (ASW) measured using DSC at 1 atm [9]. The glass transition temperature and crystallization boundary refer to the results at 1 GPa.

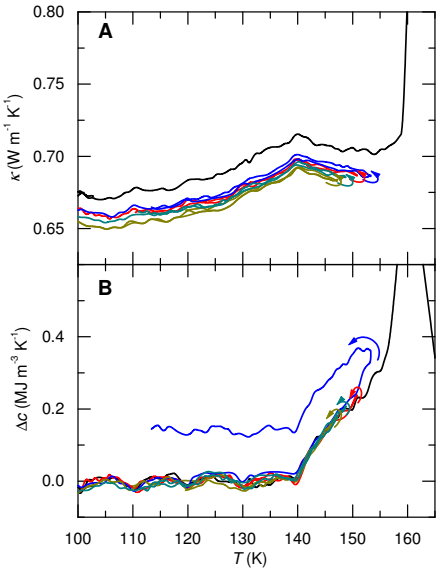

Fig. S4. Temperature cycling of water with 0.5 mol% THF (see text) at 1 GPa. (*A*) Thermal conductivity and (*B*) Excess heat capacity per unit volume plotted against temperature: Third heating cycle to a temperature in the range 147-148 K (dark yellow curve), heating cycle to 149 K (dark cyan curve), heating cycle to 151 K (red curve), and final heating cycle to 153.5 K (blue curve) during which crystallization caused a thin ice layer on the probe, which gives an anomalous irreversible increase of the heat capacity, whereas the thermal conductivity is essentially unaffected. The black curve show results for pure water on continuous heating at 0.4 K/min. (The 3% lower κ for water with 0.5 mol% THF than pure water is just outside the experimental error and indicate that the THF molecules slightly increase the phonon scattering.)

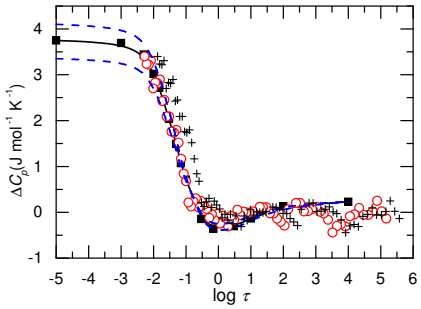

Fig. S5. Heat capacity change as a function of the logarithm of the relaxation time (in s): (+) results of measurements plotted against the dielectric relaxation time and (○) the same data but shifted △log τ=-0.4 to coincide with the calculated values (■) (see text). The dashed lines provide an error estimate.

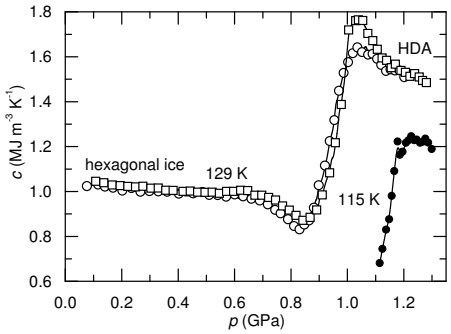

Fig. S6. Heat capacity per unit volume plotted against temperature pressure at 129 K and 115 K. The 115 K data, which have not been previously published, were obtained using a 0.1 mm hot-wire probe in a study in 2004 [11]. The 0.1 mm probe gives erroneous results for ice Ih due to the high thermal diffusivity, and the low-pressure data have therefore been removed.